

# A computational evaluation of MoS<sub>2</sub>-based materials for the electrocatalytic oxygen reduction reaction

Junyu Chen,<sup>a</sup> Jiamu Cao,<sup>a,b,c,\*</sup> Jing Zhou,<sup>a,\*</sup> Weiqi Wang,<sup>a</sup> Yufeng Zhang,<sup>a,b,c,\*</sup> Junfeng Liu,<sup>a</sup> and Xiaowei Liu<sup>a,b,c</sup>

<sup>a</sup>*School of Astronautics, Harbin Institute of Technology, Harbin, China.*

<sup>b</sup>*Key Laboratory of Micro-systems and Micro-Structures Manufacturing, Ministry of Education, 150001, China.*

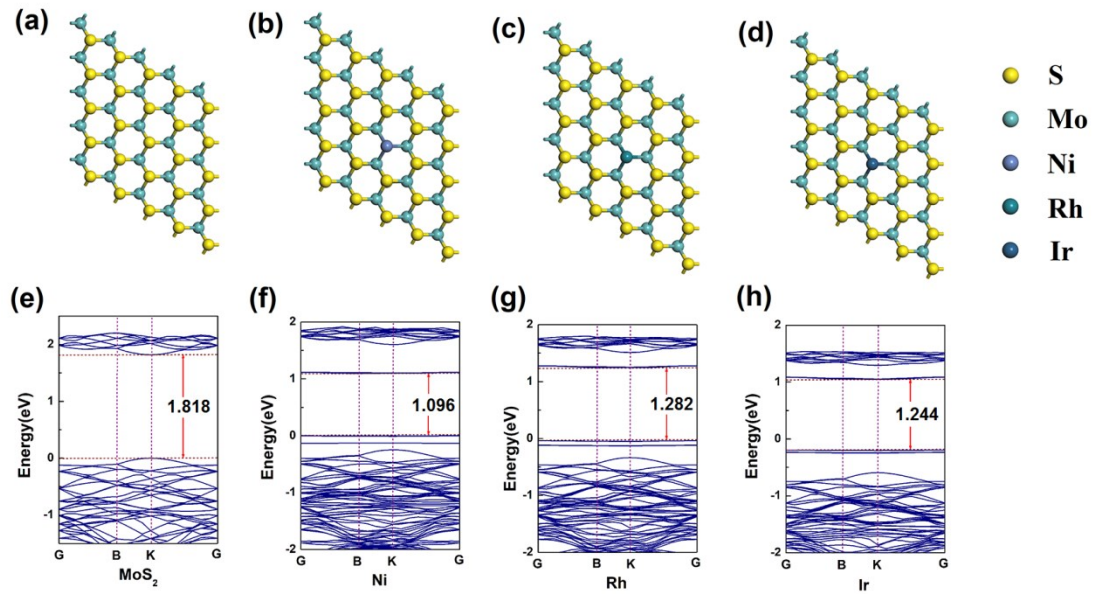
<sup>c</sup>*MEMS Center, Harbin Institute of Technology, 150001, China.*

\*corresponding author

E-mail: caojiamu@hit.edu.cn (J.M. Cao)

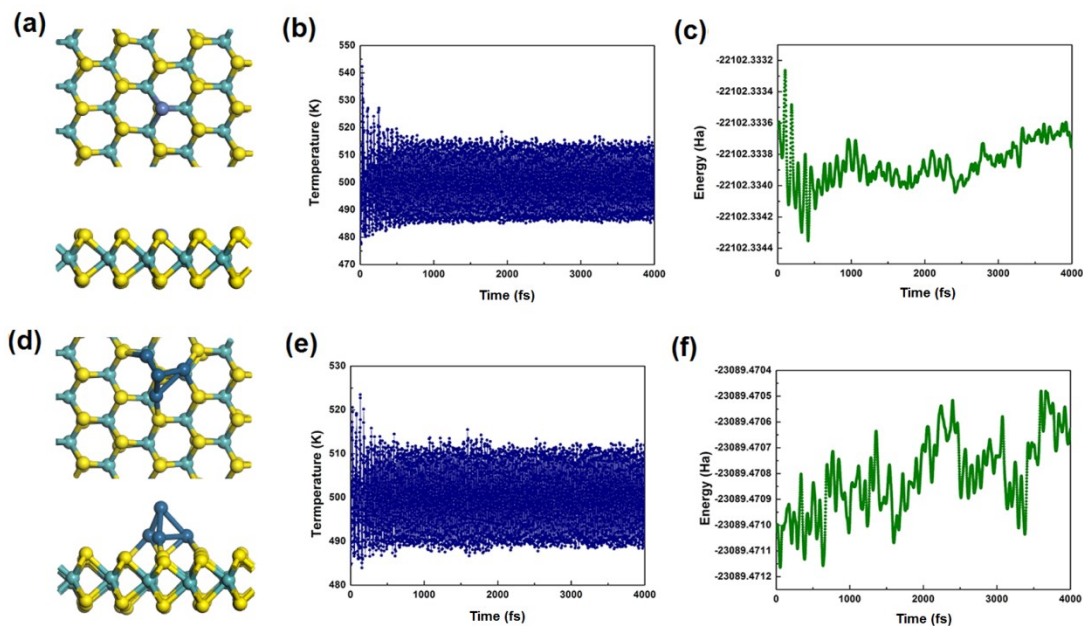
E-mail: daxiongmao@hit.edu.cn (J. Zhou)

E-mail: yufeng\_zhang@hit.edu.cn (Y.F. Zhang)



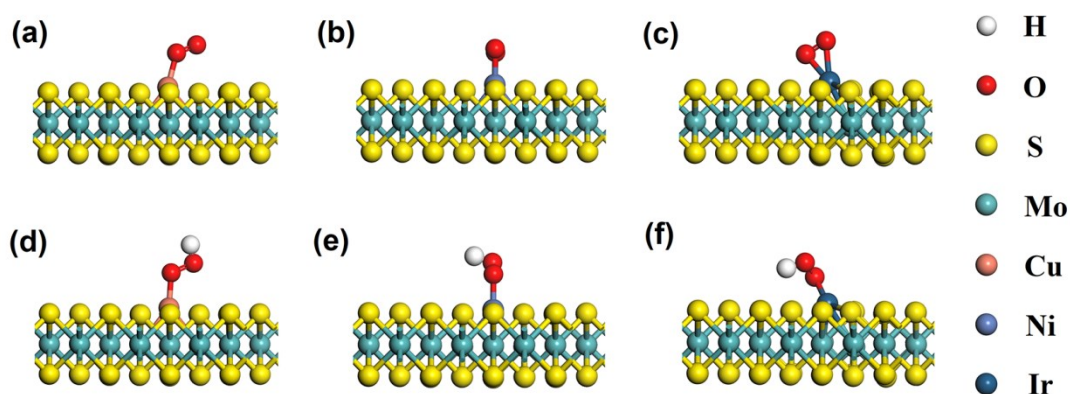
**Fig.S1** Atomic structure of (a) pristine MoS<sub>2</sub> (b) Rh-doped MoS<sub>2</sub> (c) Ni-doped MoS<sub>2</sub> (d) Ir-doped MoS<sub>2</sub>; and band structure of (e) pristine MoS<sub>2</sub> (f) Rh-doped MoS<sub>2</sub> (g) Ni-doped MoS<sub>2</sub> (h) Ir-doped MoS<sub>2</sub>.

Figure S1 presents the geometry configurations and band structures of pristine MoS<sub>2</sub> and other doped MoS<sub>2</sub> that have not been demonstrated in Fig.1. The bond length between the dopant atom and Mo atoms varies from 2.52Å to 2.65Å for doped MoS<sub>2</sub>, which were close to the S-Mo bond's 2.42Å. For the 4Pt-loaded MoS<sub>2</sub>, the Pt-S bonds vary from 2.36Å to 2.41Å. All the dopant atoms bonded well with the atoms in the material. The band structure results show that the addition of dopant atoms could bring new states to the forbidden bands and improve the conductivity of MoS<sub>2</sub>.

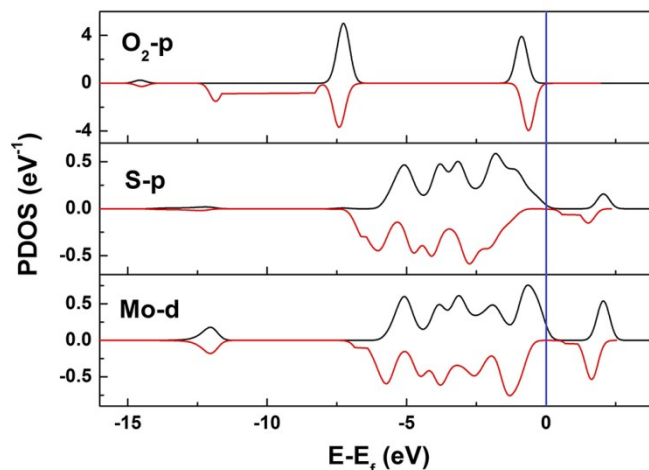


**Fig.S2** Geometry configuration after 4000 steps of (a) Ni-doped MoS<sub>2</sub> (d) 4Pt-deposited MoS<sub>2</sub>; Temperature fluctuation of (b) Ni-doped MoS<sub>2</sub> (e) 4Pt-deposited MoS<sub>2</sub>; Total energy change of (c) Ni-doped MoS<sub>2</sub> (f) 4Pt-deposited MoS<sub>2</sub>.

Figure S2 demonstrated the molecular dynamics (MD) simulation results of Ni-doped MoS<sub>2</sub> and 4Pt-deposited MoS<sub>2</sub>. From the geometry results, it could be found that after 4000fs at 500K, the Ni-doped MoS<sub>2</sub> has no evident structural change. For the 4Pt-deposited one, the Pt atoms have some displacement, while they still closely adsorbed on the surface of MoS<sub>2</sub>. From the energy results, there is no significant energy charge for these two structures during the process. Thus, the two structures could be considered to be stable thermodynamically.



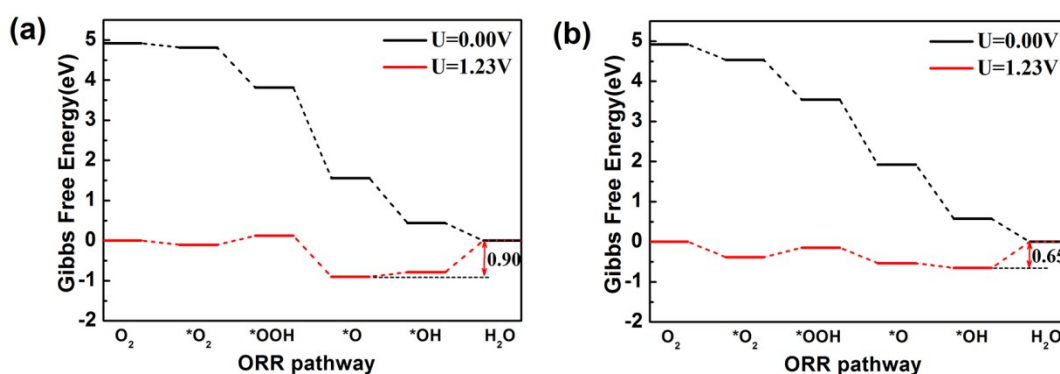
**Fig.S3** Lowest energy configurations of O<sub>2</sub> on (a) Cu-doped MoS<sub>2</sub> (b) Ni-doped MoS<sub>2</sub> and (c) Ir-doped MoS<sub>2</sub>; OOH\* on (d) Cu-doped MoS<sub>2</sub> (e) Ni-doped MoS<sub>2</sub> and (f) Ir-doped MoS<sub>2</sub>



**Fig.S4** Computed projected density of states (PDOS) of O<sub>2</sub> adsorbed on pristine MoS<sub>2</sub> surface.

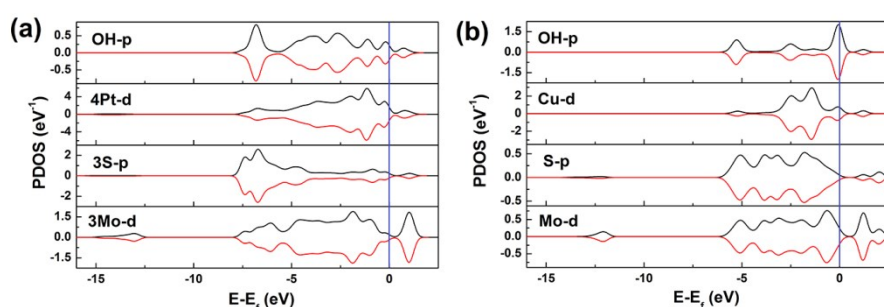
The charge transfer mechanism between an adsorbate and materials could be determined by mixing the molecular HOMO and LUMO with the orbitals of the atoms in materials [1]. It could be judged by the relationship between the Fermi level of the materials and the HOMO and LUMO levels of adsorbates. From the DFT calculation results, the HOMO level and LUMO level of a single O<sub>2</sub> molecule is -6.879eV and -4.594eV, respectively. It is comparing with the Fermi Levels  $E_f$  of these catalytic materials (Table 1). It could be found that all the  $E_f$  values were between the HOMO level and the LUMO level of an O<sub>2</sub> molecule. That indicates the charge transfer between an O<sub>2</sub> molecule, and these materials mainly depend on the orbital mixing theory [2].

Figure S4 presented the PDOS of the pristine MoS<sub>2</sub> surface when O<sub>2</sub> molecule adsorbed. It could be found that there are no evident peak overlaps between the PDOS of O<sub>2</sub> and MoS<sub>2</sub>. Indicating the orbital mixing between O<sub>2</sub> molecule and pristine MoS<sub>2</sub> is weak.



**Fig.S5** Schematic Gibbs free energy diagrams of ORR on the (a), 2Pt-deposited MoS<sub>2</sub> (b) 7Pt-deposited MoS<sub>2</sub>

Figure S5 shows the Gibbs free energy diagrams of the ORR process on 2Pt- and 7Pt-deposited MoS<sub>2</sub>. The results reveal that the total overpotential of 2Pt-deposited MoS<sub>2</sub> is 0.90eV, which is inferior to that of the 4Pt-deposited one. While that of 7Pt-deposited MoS<sub>2</sub> is 0.65eV, even better than pure Pt (0.68eV). These results indicate that the depositing content of Pt easily influences the catalytic activity of Pt-deposited MoS<sub>2</sub>. But it is mentionable that Pt-deposited MoS<sub>2</sub> has the potential to have better ORR catalytic activity than pure Pt. Further studies are expected to optimize this Pt-deposited MoS<sub>2</sub> for ORR applications.



**Fig.S6** Computed projected density of states (PDOS) of OH adsorbed on (a) 4Pt-loaded MoS<sub>2</sub>  
(b) Cu-doped MoS<sub>2</sub>

Figure S6 showed the whole PDOS when OH adsorbed on 4Pt-loaded MoS<sub>2</sub> and Cu-doped MoS<sub>2</sub>. It could be found there are several overlaps of DOS between OH and the dopant atoms, such as the 4Pt-loaded one at -6.9eV and -1.3eV, the Cu-doped one at -2.5eV and 0eV. The OH species bonded well with the materials.

**Table S1** Primitive values of intermediate quantity of  $E_{\text{form}}$

Materials	$E_{\text{X-MoS}_2}$ (Ha)	$E_{\text{MoS}_2}$ (Ha)	$E_{\text{X}}$ (Ha)	$E_{\text{host}}$ (Ha)
Cu-MoS <sub>2</sub>	-22119.7277006		-444.9117939	
Rh-MoS <sub>2</sub>	-22040.9639438		-287.2875427	
Ni-MoS <sub>2</sub>	-22090.7540116		-386.8678644	
Ir-MoS <sub>2</sub>	-22075.1500543	-22295.3548080	-355.6566241	-398.0380858
Co-MoS <sub>2</sub>	-22064.0584944		-333.5050130	
N-MoS <sub>2</sub>	-21951.9447713		-109.4491128	

**Table S2** Primitive values of adsorption energy to reaction intermediates  $E_{\text{ads}}$ 

Materials	$E_{\text{substrate}}$ (Ha)	$E_{\text{system}}$ (Ha)			
		O <sub>2</sub>	OOH	O	OH
MoS <sub>2</sub>	-22295.354809	-22445.579299	-22446.186468	-22370.497497	-22371.071891
Cu-MoS <sub>2</sub>	-22119.727701	-22270.005047	-22270.633420	-22194.849648	-22195.531593
Rh-MoS <sub>2</sub>	-22040.963944	-22225.448150	-22226.051221	-22150.325831	-22150.945799
Ni-MoS <sub>2</sub>	-22090.754012	-22191.258373	-22191.865542	-22116.114452	-22116.754942
Ir-MoS <sub>2</sub>	-22075.150054	-22225.448149	-22226.051221	-22150.325831	-22150.945799
4Pt-MoS <sub>2</sub>	-21951.944771	-23227.014528	-23227.637619	-23151.893410	-23152.534069
Pure Pt	-7034.430010	-7184.704819	-7185.317651	-7109.548687	-7110.206089
Pt-MoS <sub>2</sub>	-22092.605065	-22242.869005	/	/	/
Co-MoS <sub>2</sub>	-22064.053771	-22214.364744	/	/	/
Pd-MoS <sub>2</sub>	-22060.611499	-22210.873939	/	/	/

$E_{\text{adsorbate}}$  values are -150.246707 Ha for O<sub>2</sub>, -150.828929 Ha for OOH, -75.007936 Ha for O and -75.682944 Ha for OH.

The calculated  $E_{\text{ads}}$  value for Pt-doped MoS<sub>2</sub> is -0.47eV; for Co-doped MoS<sub>2</sub> is -1.75eV; for Pd-doped MoS<sub>2</sub> is -0.43eV. All the three are not in the range of -1.4eV to -0.5eV. Indicating doping Pt, Co, or Pd atoms is not favorable for the ORR process.

**Table S3** Hirshfeld charge results of ORR species when adsorbed on catalytic materials

Materials	O <sub>2</sub>	OOH	O	OH
MoS <sub>2</sub>	0.0507	0.1137	0.2525	0.0763
Cu-MoS <sub>2</sub>	0.2146	0.1916	0.3423	0.265
Rh-MoS <sub>2</sub>	0.1667	0.0528	0.2549	0.1463
Ni-MoS <sub>2</sub>	0.0942	0.0682	0.2465	0.1482
Ir-MoS <sub>2</sub>	0.1785	0.0507	0.2044	-0.1275
4Pt-MoS <sub>2</sub>	0.1827	0.1279	0.2756	0.1629
Pure Pt	0.2202	0.0648	0.3049	0.1776

**Table S4** Primitive values of zero-point energy and entropy.

Materials	pristine		O <sub>2</sub>		OOH		O		OH	
	S	ZPVE	S	ZPVE	S	ZPVE	S	ZPVE	S	ZPVE
	(cal/m ol/K)	(kcal/ mol)	(cal/m ol/K)	(kcal/ mol)	(cal/m ol/K)	(kcal/ mol)	(cal/m ol/K)	(kcal/ mol)	(cal/m ol/K)	(kcal/ mol)
MoS <sub>2</sub>	356.01	92.98	370.29	95.13	390.35	102.19	369.47	95.24	374.24	100.22
Cu-MoS <sub>2</sub>	374.13	91.40	398.61	94.45	391.41	101.81	378.36	93.06	382.19	99.55
Rh-MoS <sub>2</sub>	374.53	91.42	380.38	95.66	389.58	101.96	379.25	93.08	382.50	99.44
Ni-MoS <sub>2</sub>	372.13	91.71	390.30	94.43	389.15	101.32	379.65	93.03	383.64	99.33
Ir-MoS <sub>2</sub>	375.91	91.27	386.09	94.70	387.41	101.94	379.49	91.09	381.24	99.74
4Pt-MoS <sub>2</sub>	409.41	94.81	423.39	97.58	428.64	101.65	419.02	96.03	420.27	102.66
Pure Pt	349.34	17.55	352.42	20.80	360.43	27.86	347.76	18.62	358.82	25.36

**Table S5**  $\Delta G$  values for each step of ORR occurred on the six kinds of materials

Materials	$\Delta G$ (eV)				
	Step (1)	Step (2)	Step (3)	Step (4)	Step (5)
Cu-MoS <sub>2</sub>	-0.4634036	-0.7689922	-0.8021236	-2.4067515	-0.4787291
Rh-MoS <sub>2</sub>	-0.5974830	-0.4500454	-1.7325706	-1.2770819	-0.8628191
Ni-MoS <sub>2</sub>	-0.7290691	-0.4518576	-1.4313767	-1.8159060	-0.4917906
Ir-MoS <sub>2</sub>	-1.0119312	-0.1959040	-2.5479899	-0.6001511	-0.5640238
4Pt-MoS <sub>2</sub>	-0.4330286	-0.7991790	-1.9173312	-1.243957	-0.5256038
Pure Pt	-0.2816292	-0.5550804	-1.2381629	-1.8211867	-1.0239407

## Reference

- [1] O. Leenaerts, B. Partoens, and F. M. Peeters, Adsorption of H<sub>2</sub>O, NH<sub>3</sub>, CO, NO<sub>2</sub>, and NO on graphene: A first-principles study *Phys. Rev. B* **2008**, *77*, 125416
- [2] Zhou, C. J.; Yang, W. H.; Zhu, H. L., Mechanism of Charge Transfer and Its Impacts on Fermi-Level Pinning for Gas Molecules Adsorbed on Monolayer WS<sub>2</sub>. *Journal of Chemical Physics* **2015**, *142*.